Assisted drop evaporation: a new route for the formation of nanoparticle deposits

Carmen Lucía Moraila-Martínez, Miguel Cabrerizo-Vílchez and Miguel Ángel Rodríguez-Valverde
Department of Applied Physics, Campus Fuentenueva s/n, University of Granada, 18071 Granada, Spain
Corresponding author: cmoraila@ugr.es
http://www.ugr.es/local/marodri/complexfluids.php, http://biocol.ugr.es/

Keywords: drop evaporation, contact line dynamics, shrinking drop, receding contact angle

1 Introduction

Moving droplets are an efficient way of transporting and/or collecting sensitive and fragile material such as cells, nanotubes, and different micro/nano-objects. Desiccation of colloidal drops appears in many applications such as inkjet printing, bioassay manufacturing, colloidal assembly/templating, micro and nanowires fabrication, nanocrystals, cosmetics and microelectronics [1]. In this scenario, ring/stain formation of drying colloidal suspensions is ruled by contact line dynamics [2]. Receding contact lines are ubiquitous at evaporating drops but the time scale of the process is extremely long. The analysis of dry drops is usually performed only after the complete drying (evaporation of loosely bound water).

During the evaporation of a sessile drop, before the backward movement of contact line, a receding contact angle (θ_r) is hold. Rigorously, receding mode corresponds to the incipient relative motion of three-phase contact lines on solid surfaces. In practice, the reproducibility of experiments with evaporating drops is poor. Kinetics of freely evaporating drop is very long since evaporating drops undergo a minimum rate of liquid loss. Furthermore, there is a strong influence on the receding contact angle value from the rate of liquid removal from the drop. When an evaporating drop recedes very slowly, it may be trapped at the first local energy minimum that is encountered.

Generally, evaporation of simple liquids can occur in two distinct modes, at a constant contact angle and varying contact radius or vice versa [3]. In the constant contact angle mode, it has been found that the liquid-vapour area, A_{LV}, decreases linearly with time [4]. If a sessile drop is slowly shrinking with constant contact angle, the following rule should be hold:

$$\frac{dA_{LV}}{dt} = \frac{dA_{SL}}{dt}\cos\theta_r \tag{1}$$

where A_{SL} is the solid-liquid area. From Eq. 1, if $A_{LV} \propto (t_0 - t)$ then $r_c^2 \propto (t_0 - t)$, as well. The time t_0 stands for the transition time between the fixed contact line mode and the constant contact angle mode. For spherical drops, the volume scales with contact radius as $V \propto r_c^3$. If this scaling applies to gravity-flattened drops, we predict that $V \propto (t_0 - t)^{3/2}$ for the constant contact angle mode of drop evaporation. In fact, this result agrees with the evaporation rate of a receding drop:

$$-\frac{dV}{dt} \propto \sqrt{t_0 - t} \tag{2}$$

whereas the loss rate of volume for a sessile drop with fixed contact line is:

$$-\frac{dV}{dt} = const. \tag{3}$$

With a variable rate of withdrawal of liquid [5], we are able to control the speed of the receding contact line and further, to emulate the main stages of drop evaporation (see Table 1), at shorter times. This approach allows to standardize the contact line dynamics of evaporating drops.

	Flow rate	Liquid-vapor area	Contact radius	Contact angle
Static shrinking drop	Steady	–	Constant	$> \theta_r$
Receding shrinking drop	Square-root	$\propto (t_0 - t)$	$\propto \sqrt{t_0 - t}$	θ_r

Table 1: Contact line dynamics as the volumetric flow rate imposed during the assisted drop evaporation.

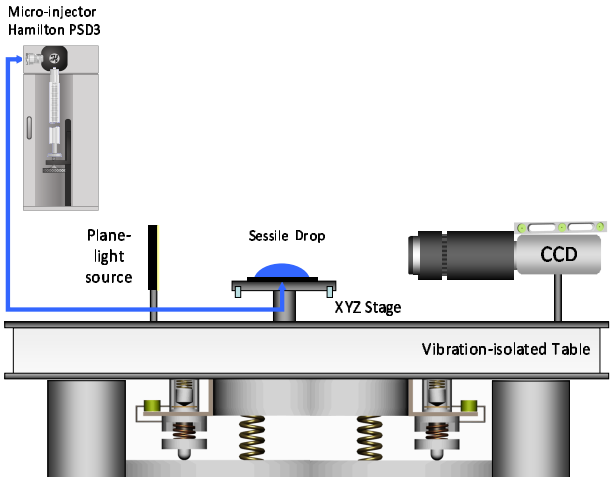

Figure 1: Experimental device used for the assisted drop evaporation.

2 Materials and methods

We performed the *assisted drop evaporation* using the technique known as low-rate dynamic contact angle [6]. In this technique, a small hole was drilled in the substrate sample and a tube was connected to this hole beneath the substrate. The drop volume was then changed by removing liquid to a initial drop by means of the tube connected to a motorized micrometer syringe (Hamilton© PSD3). With this technique, the liquid was suctioned from the bulk. Hence, the flux distribution created was apparently different to the flux generated within a free evaporating drop. However, in this work, we just intended to mimic the contact line dynamics of evaporating drops at shorter times (100-600 s).

Commonly, low-rate dynamic contact angle measurements are achieved with a continuous linear variation of drop volume (see Eq. 3). Instead, in order to reproduce the constant contact angle mode of evaporating drops, we used a non-linear variation of drop volume (as Eq. 2).

The experimental set-up used for the contact angle measurements is showed in Figure 1. Due to the limitations of stepper-motor-driven syringe pumps, our strategy was based on the discontinuous variation of drop volume in time at decreasing motor speeds. This way, we were able to control the volumetric flow rate of retraction of the liquid. We divided each shrinking mode into small liquid withdrawals, which were reproduced at steady flow rate following the law (2). We assured that the capillary number of the contact line was small enough ($Ca \approx 10^{-6}$). Moreover, the time between each removal of liquid was always greater than the interfacial relaxing time of drop. Hence, the shrinking drop was not altered by Hydrodynamics. Due to the drop dimensions, a microscope (Leica© Apo-Zoom) was coupled to a SONY© CCD (Charge Couple Device) camera. The interface is light-contrast illuminated using a plane and homogeneous light source (Dolan Jenner QVABL). The video image signal was digitalized with a video card connected (Data Translation DT3155) to a PC. Once the image was digitalized, the detection process provided a set of points that represented the drop profile. We applied the technique Axisymmetric Drop Shape Analysis-Profile to extract the contact angle and contact radius of drop [7]. The maximum volume of drop was chosen 220 μl. The purpose of choosing relatively large drops was to avoid any possible line tension effects on the measured contact angles and to assure the observation of receding contact angle.

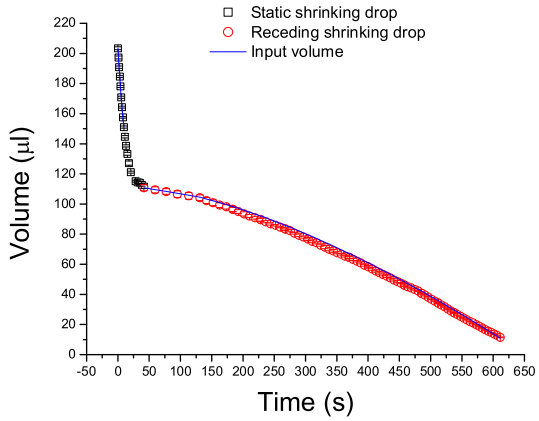

(a) Drop volume in terms of time

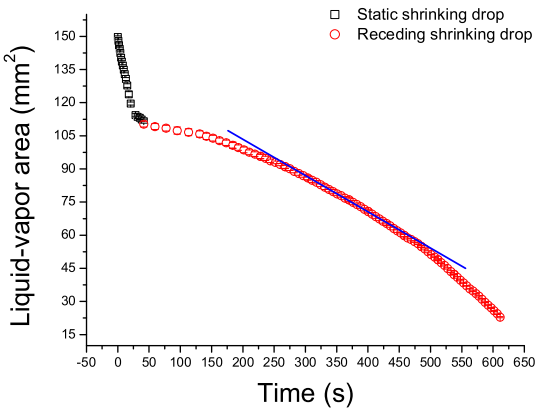

(b) Liquid-vapour area in terms of time

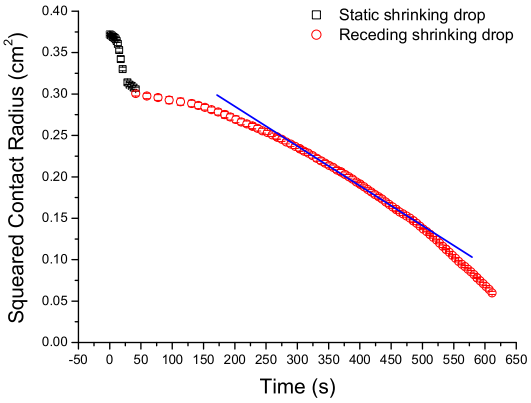

(c) Squared contact radius in terms of time

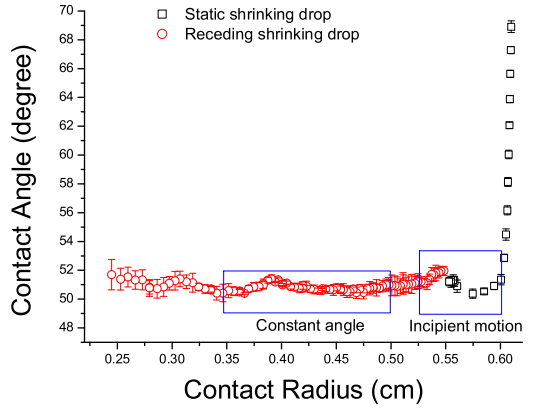

(d) Contact angle in terms of contact radius

Figure 2: Experiment of assisted drop evaporation on a PMMA surface. We illustrate the linear behaviour of the liquid-vapour area and the squared contact radius, with blue straight lines.

The experiments of assisted drop evaporation were performed in open air conditions (22^{o}C and 55% RH) with Milli-Q water on smooth PMMA surfaces (2mm-thickness, CQ grade, GoodFellow), as provided by the supplier ($R_a = 80$nm and $R_q = 120$nm).

3 Results

In Figure 2, we show a typical experiment of assisted drop evaporation performed following our approach. We observed that the liquid-vapour area decreased linearly as time for an intermediate range (see Figure 2b), after the fixed contact line mode. As expected, the three-phase contact radius was a non-linear function of time (see Figure 2c). Consequently, the volume-contact radius scaling $V \propto r_c^3$ was validated for large drops. As happens with freely evaporating drops, the unsteadily moving contact lines held a constant contact angle (see Figure 2d). We also carried out short and long experiments (100 s and 600 s, respectively) with the assisted drop evaporation (see Figure 3). In the short experiment, no hydrodynamics effects were found (see Figure 3b). Above 600 s, the shrinking drop began to evaporate because the withdrawal rate was similar to the actual evaporation rate.

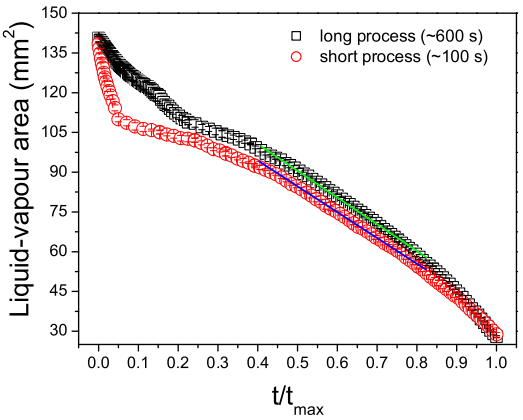

(a) Liquid-vapour area in terms of normalized time

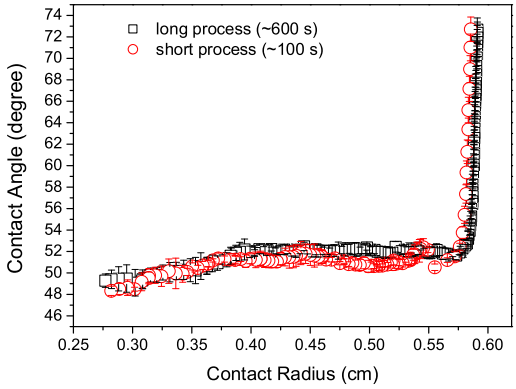

(b) Contact angle in terms of contact radius

Figure 3: Short and long experiments of assisted drop evaporation on a PMMA surface. We illustrate the linear behaviour of the liquid-vapour area with blue and green straight lines for each experiment.

4 Conclusions

Contact line dynamics of sessile drops was controlled by regulating the volume flow rate in low-rate dynamic contact angle experiments. The overall process of liquid drop evaporation, including the final mixed stage (see Figure 3b), was successfully reproduced at shorter times. Our method was independent on the process length, up to 600 s. Unlike the meniscus geometry (dip coating), experiments with sessile drops [8] allow us analyzing the effect of the curvature on the colloid confinement at the three-phase contact line. In forthcoming research, we will focus on receding contact lines of complex liquid drops, stick-slip phenomena and colloidal patterning. The assisted drop evaporation allows examining separately the impact of contact line dynamics and internal flow of evaporating drops, because the flux distribution imposed is the same for all experiments.

Acknowledgments

This research work has been supported by the "Ministry of Science and Innovation" (project MAT2010-14800) and by the "Junta de Andalucía" (projects P07-FQM-02517, P08-FQM-4325 and P09-FQM-4698).

References

1. A.-M. Cazabat and G. Guna, *Soft Matter* **6**, 2591-2612 (2010).
2. R.D. Deegan, O. Bakajin, T. F. Dupont, G. Huber, S. R. Nagel and T. A. Witten., *Nature* **389**, 827-829 (1997).
3. H. Yildirim Erbil, G. McHale, S. M. Rowan, and M. I. Newton, *Langmuir* **7**, 7378-7385 (1999).
4. H. Yildirim Erbil, G. McHale, and M. I. Newton,*Langmuir* **21**, 26362641 (2002).
5. H. Tavana and A.W. Neumann,*Colloids and Surfaces A: Physicochemical and Engineering Aspects* **282-283**, 256-262 (2006).
6. D. Y. Kwok, C. J. Budziak and A. W. Neumann, *Journal of Colloid and Interface Science* **173**, pp 143-150 (1995).
7. P. Cheng, A. Neumann, *Langmuir* **62**, 297305 (1992).
8. E. Rio, A. Daerr, F. Lequeux, and L. Limat., *Langmuir* **22**, 3186-3191 (2006).